PROCEEDINGS OF SCIENCE

# Uncertainties on $H$ and $t\bar{t}$ Predictions at the LHC (and update on Intrinsic Charm)

**Carl Schmidt*[a], Sayipjamal Dulat[b], Jun Gao[c], Marco Guzzi[d], Tie-Jiun Hou[e], Joey Huston[a], Jon Pumplin[a], Pavel Nadolsky[c], Daniel Stump[a], and C.-P. Yuan[a]**

[a] *Department of Physics and Astronomy, Michigan State University, East Lansing, MI 48824 USA*
[b] *School of Physics Science and Technology, Xinjiang University,Urumqi, Xinjiang 830046 China*
[c] *Department of Physics, Southern Methodist University, Dallas, TX 75275-0181, USA*
[d] *Deutsches Elektronen-Synchrotron DESY, Notkestrasse 85, D-22607 Hamburg, Germany*
[e] *Institute of Physics, Academia Sinica, Taipei, Taiwan 115*
*E-mail:* schmidt@pa.msu.edu

We report on a recent study of the possibility of intrinsic (non-perturbative) charm in parton distribution functions (PDFs) of the proton, within the context of the CT10 next-to-next-to-leading order (NNLO) global analysis. We also report on a study of uncertainties in the production of the Higgs boson and $t\bar{t}$ through gluon fusion at the LHC, arising from uncertainties of the PDFs and of the value of the strong coupling constant $\alpha_s(M_Z)$. Comparison is made between the predictions of the uncertainties computed based on the Hessian and the Lagrange Multiplier methods within the CTEQ-TEA global analysis framework. CT10 IC (intrinsic charm) PDF sets and CT10H (Higgs boson extreme uncertainty) PDF sets are publicly available for model-specific phenomenological analyses.

*XXII. International Workshop on Deep-Inelastic Scattering and Related Subjects,*
*28 April - 2 May 2014*
*Warsaw, Poland*

*Speaker.

 

PoS(DIS2014)146

## 1. Constraints on Intrinsic Charm from CTEQ-TEA global analysis

The most recent publicly-available PDF sets obtained from next-to-next-to-leading order (NNLO) analysis by the CTEQ-TEA group are the CT10NNLO PDFs (referred to as CT10 here) [1]. In conjunction with this global analysis a study of constraints on the charm quark mass resulted in a preferred value of $m_c(m_c) = 1.15^{+0.18}_{-0.12}$ GeV at the 68% confidence level (C.L.) [2]. Motivated by these studies, we have reconsidered the possibility of a nonperturbative (intrinsic) charm content in the PDFs in the context of the CT10 global analysis [3]. This updates an earlier intrinsic charm PDF analysis, based on CTEQ6.5 PDFs [4], with the most important improvements being the use of NNLO theory and the use of more recent data, particularly the combined H1/ZEUS data for deep-inelastic scattering [5] and inclusive charm production [6] at HERA.

Using a charm pole mass of $m_c = 1.3$ GeV, compatible with the value discussed above, we considered two model intrinsic charm distributions, defined at the initial scale $Q_c = 1.3$ GeV. The SEA model is parametrized by a "sea-like" nonperturbative function, proportional to the sum of the initial up and down sea quarks. The BPHS model is parametrized by a "valence-like" nonperturbative function based on work by Brodsky, Hoyer, Peterson, and Sakai [7]. Both models have an unfixed overall normalization parameter, which we can specify by the momentum fraction carried by the intrinsic charm content, $\langle x \rangle_{\rm IC}$, defined at the scale $Q_c$.

In Fig 1 we plot the global chi-square function $\chi^2_F$ versus $\langle x \rangle_{\rm IC}$ for the two different models of intrinsic charm. In this plot we also show dashed curves that include "Tier-2" penalties [3], designed to ensure that no individual data set is too poorly fit. The four dots in this figure correspond to exemplary fits with $\langle x \rangle_{\rm IC} \lesssim 0.57\%$ and 2% for the BHPS models and 0.57% and 1.5% for the SEA models. These four PDF fits are publicly available as CT10 IC PDFs. From this analysis we have obtained upper limits at 90% C.L. of $\langle x \rangle_{\rm IC} \lesssim 0.025$ for the BHPS model and $\langle x \rangle_{\rm IC} \lesssim 0.015$ for the SEA model.

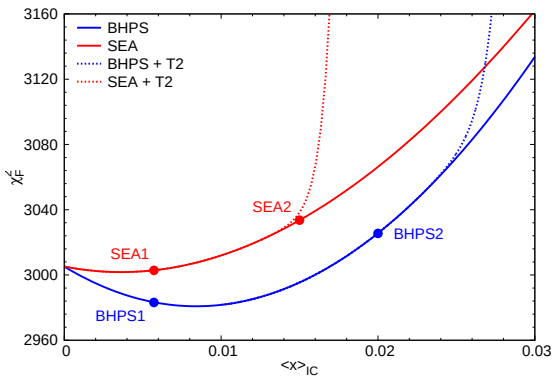


**Figure 1:** The global chi-square function $\chi^2_F$ (with and without Tier-2 penalties) versus charm momentum fraction, $\langle x \rangle_{\rm IC}$.

We have studied the impact of nonzero intrinsic charm on $W$ and $Z$ production and on Higgs and $t\bar{t}$ production at the LHC. For the most part the predictions are within the current CT10 PDF uncertainty, although precise data may eventually favor either the SEA or BHPS models. The process $pp \to Zc$ is particularly sensitive to "valence-like" intrinsic charm, since it would produce an enhancement at high $Z$ boson transverse momentum.

## 2. Uncertainties in Higgs and $t\bar{t}$ production

Since a precise determination of the Higgs boson cross section in gluon fusion is crucial for determining the Higgs boson properties, it is necessary to understand all contributions to the uncer-

tainties in the predicted cross section, including that due to PDF and $\alpha_s$ uncertainties. A standard method for calculating these uncertainties is the Hessian Method, which uses a set of error PDFs (usually twice the number of PDF parameters) to calculate the uncertainty, and assumes a quadratic dependence of the $\chi^2$ and a linear dependence of the cross section on the PDF parameters. To check the validity of these uncertainty calculations, we have performed a comparison analysis between the Hessian method and the Lagrange Multiplier (LM) method for obtaining the uncertainty of the $gg \to H$ cross section at NNLO in the context of the CT10 global analysis. The LM uncertainty is more robust, making no assumptions on the parameter dependence; however, it is more complicated to calculate, since it requires computing a constrained PDF global minimization as a function of the observable values. Consequently, it must be redone for each observable of interest.

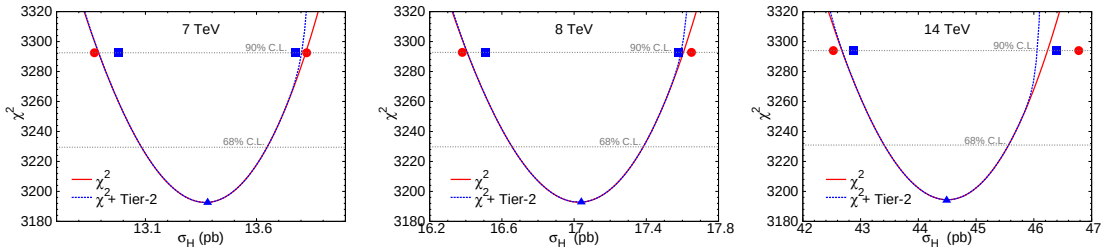


**Figure 2:** $\chi^2$ versus $\sigma_H$ with $\alpha_s(M_Z) = 0.118$. The constrained minimum of $\chi^2$ is plotted as a function of the predicted cross section $\sigma_H$ for Higgs boson production via gluon fusion channel at the LHC, for $\sqrt{s} = 7, 8$ and 14 TeV. The constrained fits without and with the Tier-2 penalties are shown as red solid and blue dashed curves, respectively. The red circles and blue boxes indicate the 90% CL errors obtained from the Hessian method without and with the Tier-2 penalties, respectively.

In Fig. 2 we show the predictions for uncertainties in the cross section at three LHC center-of-mass energies, 7 TeV, 8 TeV, and 14 TeV, assuming a fixed value of $\alpha_s(M_Z) = 0.118$. The curves are calculated using the LM method, while the circles and squares are calculated in the Hessian method at the 90% C.L., corresponding to a $\Delta\chi^2$ tolerance of 100. The red values are using just the global $\chi^2$, and the blue values are using $\chi^2$ plus Tier-2 penalties to obtain constraints. Although we see some small differences in the uncertainty estimates, as well as differences in the asymmetry of the estimates, these differences are considerably smaller than the errors themselves. Thus, we expect that the Hessian predictions, for this observable, to be reliable.

In the Hessian method, the combined PDF+$\alpha_s$ uncertainty is calculated by including two additional error PDFs, again assuming quadratic dependence of $\chi^2$ on the PDF parameters and on $\alpha_s$. In the LM method it is possible to include the uncertainty in $\alpha_s$ directly as a contribution to the total $\chi^2$. Using the PDF4LHC [9] choice of $\alpha_s(M_Z) = 0.118 \pm 0.002$ at 90% C.L., we can then obtain the correlated error ellipses between the different values of the Higgs cross section and values of $\alpha_s(M_Z)$. These are shown in Fig. 3, where we display contour plots of the total $\chi^2$ (including Tier-2 penalties) in the $(\alpha_s, \sigma_H)$ plane for LHC center-of-mass energies 7 TeV, 8 TeV, and 14 TeV. The thick black outer and inner contours correspond to 90% C.L. and 68% C.L. The departure from pure ellipses in these curves is indicative of non-quadratic dependence on the PDF parameters. It is particularly evident in the 14 TeV contour, where the Tier-2 penalty has a large effect on the upper part of the contour. Nevertheless, the uncertainties calculated by the Hessian

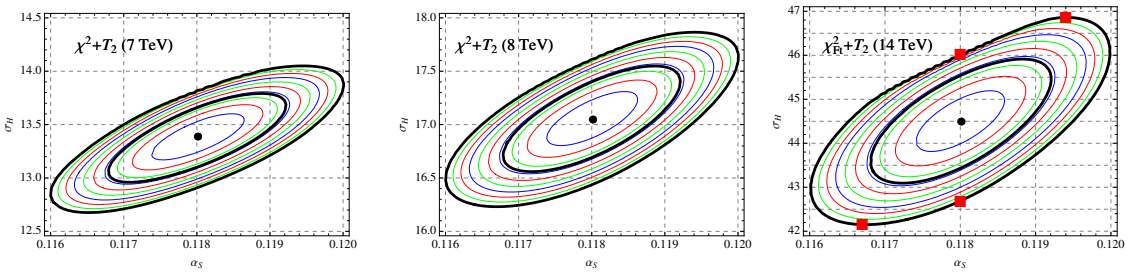


**Figure 3:** Contour plots of $\chi^2 + T_2$ in the $(\alpha_s, \sigma_H)$ plane, for $\sigma_H$ (in pb unit) at the LHC, with 7, 8 and 14 TeV. The thick black outer and inner contours are at $\Delta\chi^2 = 100$ and $100/(1.645)^2$, respectively, for the 90% CL and 68% CL. The thin colored contours are at intervals in $\chi^2$ of 10. The fits that give minimum and maximum $\sigma_H$ are indicated by the red square symbols, with $\alpha_s(M_Z) = 0.1167, 0.118$ or $0.1194$.

and the LM methods still agree well. For instance, we obtain the 90% C.L. uncertainties (PDF+$\alpha_s$) for the Higgs cross section through gluon fusion at the 14 TeV LHC to be $+5.2/-5.2$ in the LM method and $+5.4/-5.0$ in the Hessian method (given as % of the central value).

We have made publicly available the PDF sets (called CT10H) that give the extreme values of the Higgs cross section at 90% C.L. for the LHC center-of-mass energy 14 TeV. These correspond to the red squares on the right-hand plot of Fig. 3. These include two extreme sets for fixed $\alpha_s(M_Z) = 0.118$ and two extreme sets for varying $\alpha_s$, corresponding to $\alpha_s(M_Z) = 0.1167$ and $\alpha_s(M_Z) = 0.1194$ for minimum and maximum $\sigma_H$, respectively. These extreme sets can be useful for making efficient error analyses of the Higgs boson cross section. Although these PDF sets were obtained using $\sigma_H$ at 14 TeV, they also give good predictions for the uncertainty at the other energies, because the error dependence on the cross section is strongly correlated over this range of energies.

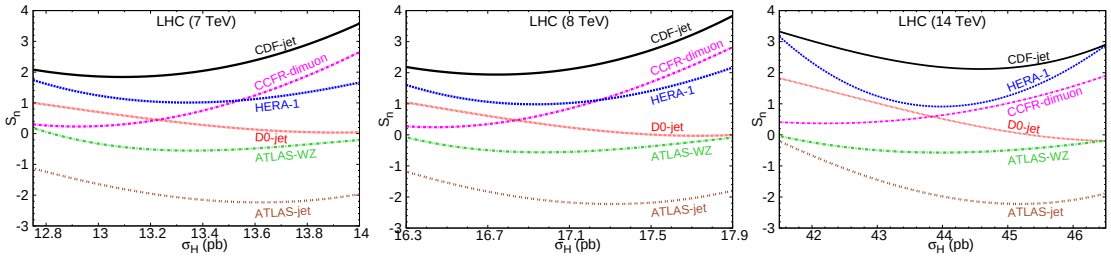


**Figure 4:** The equivalent Gaussian variable $S_n$ versus $\sigma_H$ (in pb unit) at the LHC, with 7, 8 and 14 TeV, for the several different data sets.

While performing the LM analysis, we were able to observe the sensitivity of the different data sets to different values of the Higgs cross section, as shown in Fig. 4. For this, we defined an "Effective Gaussian Variable" $S_n$, which maps the cumulative $\chi^2$ distribution for the $N_{pt}$ data points onto a cumulative Gaussian distribution, in order to easily see the compatibility of any given data set with a particular value of $\sigma_H$. Values of $S_n$ between -1 and +1 correspond to a good fit (at the 68% C.L.), large positive values ($\gtrsim 2$) correspond to poor fit, while large negative values

($\lesssim -2$) are anomalously well-fit. See Ref. [8] for more details. The most sensitive data was found to be CDF [10] and D0 [11] high $p_T$ jet, inclusive HERA [12], and CCFR-dimuon [13] data. The inclusive HERA data is most strongly correlated at 14 TeV, where smaller $x$ values are important. The CCFR dimuon correlation can be traced to gluon-strange interdependence of the PDFs.

The consistency of Hessian and LM uncertainties must be checked on a case-by-case basis for different observables. We have performed the same analysis for the $t\bar{t}$ cross section at the LHC. Again we find small differences in size and asymmetry of the uncertainties between the two methods, but these differences are smaller than the uncertainty itself. Thus, we have verified the reliability of the Hessian method for $t\bar{t}$ at the LHC. We have also obtained extreme error sets for the $t\bar{t}$ cross section, analogous to the CT10H sets. We have verified them by calculating uncertainties in the top quark transverse momentum distribution from $t\bar{t}$ events at the 7 TeV LHC, using the approximate-NNLO program DiffTop [14]. Note that to obtain errors with the extreme sets requires just two additional PDF runs, as opposed to the much larger number needed for the Hessian error calculation. In the dominant region of $p_T \lesssim 200$ GeV, the uncertainties obtained in the two methods are very consistent, as expected. Interestingly, at high $p_T \gtrsim 200$ GeV, the extreme sets give a smaller uncertainty. This demonstrates that the very high-$p_T$ component of the $t\bar{t}$ cross section is not completely correlated with the inclusive cross section. Consequently, for this region of the distribution, the LM extreme sets do not cover the full uncertainty range.

## References


[1] Jun Gao, Marco Guzzi, Joey Huston, Hung-Liang Lai, Zhao Li, Pavel Nadolsky, Jon Pumplin, Daniel Stump, C.-P. Yuan, arXiv:1302.6246 [hep-ph].

[2] J. Gao, M. Guzzi and P. M. Nadolsky, Eur. Phys. J. C **73**, 2541 (2013) [arXiv:1304.3494 [hep-ph]].

[3] S. Dulat, T. -J. Hou, J. Gao, J. Huston, J. Pumplin, C. Schmidt, D. Stump and C. -P. Yuan, Phys. Rev. D **89**, 073004 (2014) [arXiv:1309.0025 [hep-ph]].

[4] J. Pumplin, H.-L. Lai and W.-K. Tung, Phys. Rev. **D75**, 054029 (2007).

[5] F. Aaron *et al.*, [H1 and ZEUS Collaborations], *JHEP* **1001** (2010) 109.

[6] H. Abramowicz *et al.* [H1 and ZEUS Collaborations], Eur. Phys. J. C **73**, 2311 (2013) [arXiv:1211.1182 [hep-ex]].

[7] S. J. Brodsky, P. Hoyer, C. Peterson, and N. Sakai, Phys. Lett. **B93**, 451 (1980).

[8] S. Dulat, T. -J. Hou, J. Gao, J. Huston, P. Nadolsky, J. Pumplin, C. Schmidt, D. Stump and C. -P. Yuan, Phys. Rev. D **89**, 113002 (2014) [arXiv:1310.7601 [hep-ph]].

[9] S. Alekhin, S. Alioli, R. D. Ball, V. Bertone, J. Blumlein, M. Botje, J. Butterworth and F. Cerutti *et al.*, arXiv:1101.0536 [hep-ph].

[10] T. Aaltonen *et. al.*, **CDF** Collaboration, *Phys.Rev.* **D 78** (2008) 052006.

[11] V. Abazov *et. al.*, **D0** Collaboration, *Phys.Rev.Lett.* **101** (2008) 062001.

[12] F. Aaron *et. al.*, **H1 and ZEUS** Collaboration, *JHEP* **1001** (2010) 109.

[13] M. Goncharov *et. al.*, **NuTeV** Collaboration, *Phys.Rev.* **D 64** (2001) 112006.

[14] M. Guzzi, K. Lipka and S. -O. Moch, arXiv:1406.0386 [hep-ph].